Natural Gas Conversion VIII
F.B. Noronha, M. Schmal, E.F. Sousa-Aguiar (Editors)

Preparation of Ni/SiO_2, Ni/SiO_2-CaO and Ni/SiO_2-MgO catalysts for methane steam reforming

Alano V. da Silva Neto[a], Patrícia P. C. Sartoratto[a], Maria do Carmo Rangel[b]

[a]*Instituto de Química, Universidade Federal de Goiás, Campus Samambaia 74001-970, Goiânia, Goiás, Brazil*
[b]*Instituto de Química, Universidade Federal da Bahia. Campus Universitário de Ondina, Federação. 40 170-280, Salvador, Bahia, Brazil*

The preparation of mesoporous silica-supported nickel, by adding nickel nitrate and citric acid into a colloidal dispersion of sphere-shaped silica nanoparticles, was described in this work. The promotion with calcium and magnesium caused a decrease in specific surface area but led to an improvement of both activity in methane steam reforming and selectivity to hydrogen, making the catalysts suitable for hydrogen production. The magnesium-doped catalyst is the most promising one.

1. Introduction

Steam reforming of methane, the main component of natural gas, is the most used and economical route to produce hydrogen for industrial purposes. The catalysts are often nickel-based ones, which go on severe deactivation by coke deposition. During the reaction, coke is formed at high temperatures on both nickel and on the metal-support interface, causing the loss of small metallic particles from the support [1]. Therefore, there is a demand for catalysts that can stabilize nickel particles on the support. In this sense, amorphous silica prepared by the sol-gel method is a versatile material to be used as catalyst support, since its porosity can be modulated and the stability of metal can be improved by the addition of basic promoters to the silica framework [2]. Besides, the use of organic additives in the sol-gel precursor

mixtures, such as citric acid may also enhance the metal distribution in the silica support due to their ability to coordinate metal ions [3].
Takahashi et al. have recently reported the preparation of Ni/SiO_2 catalysts using the sol-gel process and citric acid as a non-surfactant template, under acidic reaction condition [4]. The catalysts obtained showed NiO nanoparticles from 6 to 9 nm and improved textural properties for samples containing up to 30% Ni. However, the drawback of using the sol-gel acid condition is a poor structural stability of the mesoporous silica at high temperatures [5]. More recently, Lee et al. synthesized mesoporous silica framed by sphere-shaped silica nanoparticles using a base-catalyzed sol-gel reaction and citric acid as template agent [6]. The pore size of this mesoporous silica was easily controlled up to 15 nm and the materials maintained a narrow pore size distribution, high specific surface area and high pore volume at high temperatures. The highly branched structure of the colloidal silica nanoparticles gave rise to a more rigid silica framework that shrunk less during calcination. These characteristics make the material interesting to be used in the preparation of supported nickel catalysts for steam reforming of methane at high temperature conditions.
In this study, nickel supported on amorphous mesoporous silica was prepared, by incorporating nickel nitrate and citric acid into a colloidal dispersion of sphere-shaped silica nanoparticles. Calcium and magnesium promoters were also introduced into the catalyst and the structural and textural characteristics were evaluated. The methane steam reforming was selected as a model reaction for evaluating the catalysts.

2. Experimental

The catalysts were prepared by the sol-gel method [6], using nickel nitrate hexahydrate and calcium or magnesium nitrate. The synthesis was performed using tetraethoxysilane (TEOS) in alkaline conditions at a $TEOS:NH_3:H_2O$:ethanol molar ratio of 1:0.086:53.6: 40.7. The TEOS/ethanol solution was stirred vigorously at 50 °C and a NH_3/H_2O solution was added dropwise mantaining at this temperature for 3 h, resulting in a stable colloidal silica sol. Citric acid, CA, was then added to the colloidal silica sol at TEOS:CA molar ratio of 1:1, followed by vigorous stirring at room temperature, for 10 min. Then, nickel nitrate was added to the mixture that was stirred at room temperature, for additional 15 min. Alternatively, calcium or magnesium nitrate was added to the previous mixture and stirred for 15 min. The resulting sols were poured into glass recipients and dried at 70 °C for 24 h. The xerogels were calcined at 500 ^oC, for 2 h to decompose citric acid and nitrate ions and to crystallize nickel oxide. The SiNi, SiNiCa and SiNMg samples produced were calcined at 900 ^oC, for 2 h. A reference SiO_2 sample was also prepared. The nickel, calcium and magnesium contents in the samples were determined by

atomic absorption analysis, using a Perkin Elmer 5000 instrument. Nitrogen adsorption-desorption isotherms were taken in a Micromeritics ASAP 2010 instrument, on samples previously degassed at 120 ^oC for 24 h, under vacuum. The specific surface areas were calculated from the adsorption curve (BET method) and the pore size distribution curves were obtained from the desorption branch by using the Barrett–Joyner–Halenda (BJH) method. The powder X-ray diffractograms (XRD) of the samples were recorded in a Shimadzu/XRD 6000, using CuKα radiation (λ=1.54056). The crystalline phase was identified using the JCPDS (Join Committee on Powder Diffraction Standards) data.

Fourier transform infrared spectra (FTIR) of non-calcined and calcined samples were recorded in a Bomem/MB100 spectrometer in the 4000 to 400 cm^{-1} region, using a diffuse reflectance accessory. Potassium bromide was used to record the background spectra and to dilute the samples.

The TPR experiments were carried out in a Micromeritics model TPD/TPO 2900 equipment with samples previously heated under nitrogen (150 °C, 2 h). The measurements were performed from room temperature to 1000 °C at a rate of 10 °C min^{-1} using a 5% H_2/N_2 mixture.

The catalytic tests were carried out in a stainless steel fixed bed microreactor containing 0.15 g of catalyst (100 mesh size), for 6 h. The sample was heated up to 700 °C at a rate of 10 °C min^{-1}, under nitrogen flow (60 mL min^{-1}) and then reduced at this temperature under hydrogen flow (40 mL min^{-1}), for 2 h. The runs were performed at atmospheric pressure and 600 ^oC using a steam to methane molar ratio of 4. Methane (60 $mL.min^{-1}$) was mixed with nitrogen and steam to produce a mixture of 10% CH_4 and fed to reactor. The reaction conditions were chosen to achieve a conversion of 10% with a commercial catalyst (alumina-supported nickel) and to avoid any diffusion effect. The products were analyzed by on line gas chromatography.

3. Results and Discussion

The nickel content (% wt) in the solids calcined at 500 ^oC was 12.0% for SiNi and SiNiCa samples and 11.5% for SiNiMg. The calcium or magnesium contents were around 3.8%.These values are close to the expected ones. The X-ray diffraction patterns of the samples are shown in Fig. 1(a). The typical X-ray peaks of the cubic structure of nickel oxide (111, 200, 220, 311, 222) can be observed for all samples (JCPDF 78-0643). The amorphous nature of the silica matrix is evident from the broad peak at 2θ between 15° and 35°. Furthermore, minor peaks are observed in the SiNiMg sample (900 ^oC), indicating the crystallization of magnesium silicate (JCPDF 87-0061). The XRD data did not indicate the presence of nickel and calcium silicate in the samples. The X-ray line broadening of the most intense peak (200) provided the average diameter of the nickel oxide nanocrystalline domains which varied from 6.1

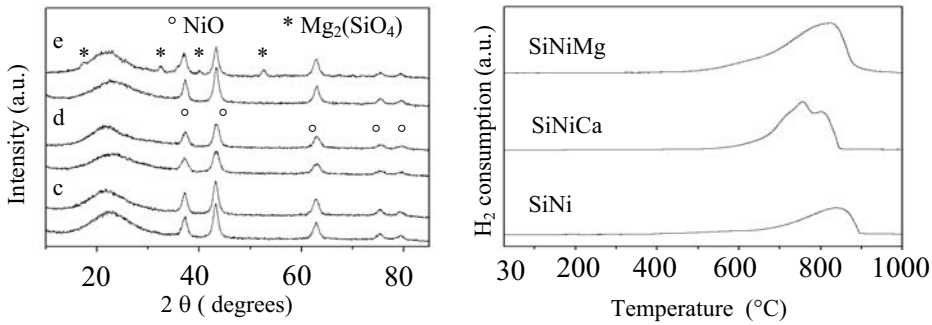

Figure 1. (a) X-ray diffractograms and (b) TPR profiles of the samples. SiNi (c), SiNiCa (d), SiNiMg (e) calcined at 500 °C (bottom) and 900 °C (top).

to 8.2 nm, as shown in Table 1. The average nanoparticle size was estimated using the Scherrer's equation [7]. The thermal treatment at 900 °C resulted in a little increase of the average diameter of the nickel oxide nanoparticles.

Before calcination, all samples showed FTIR spectra with an absorption band at 1733 cm^{-1}, assigned to carbonyl stretching (ν C=O) of citric acid and two broad absorptions (1600-1400 cm^{-1}) due to carboxylate stretching modes, indicating that citrate ions are bonded to nickel by coordinative linkages [8]. Other bands at 1100, 800 and 460 cm^{-1} due to Si-O-Si stretching (asymmetric and symmetric) and deformation modes were also noted, besides, a band at 955 cm^{-1} due to the Si-O stretching of silanol groups [9]. After calcination, the samples did not show the nitrate and carbonyl/carboxylate absorptions, indicating that these species were decomposed upon heating. The SiNiMg sample (900 °C) showed two extra bands (900, 605 cm^{-1}) attributed to Si-O-Mg stretching of magnesium silicate [10,11].

The textural properties of the samples are summarized in Table 1. The specific surface area and the pore volume of the catalyst heated at 500 °C were lower than that of silica; the SiNiCa and SiNiMg samples showed the lowest values. They decreased upon heating at 900 °C, while the average pore size and the average size of NiO crystallites did not change significantly. It means that nickel oxide, in the pores of the silica matrix, inhibits the pore collapse at high temperatures, when magnesium and calcium are absent. This can be explained by considering strong interactions between the nickel oxide nanoparticles and silanol moieties, including Si-O-Ni bonds. Furthermore, when calcium and magnesium ions were incorporated into the silica framework, the mobility of silica arrays might be enhanced, favoring the pore collapse at high temperatures. The pore size distribution was sharp regardless the calcination temperature. The presence of particle-like silica structure and citric acid before the addition of the guest ions, into the sol-gel mixture, seems to be a procedure that assures the preservation of silica mesoporous structure, for samples with up to 12% Ni.

Table 1.
Textural properties of the catalysts. hydrogen uptake in TPR experiments and coke produced during methane steam reforming.

Sample [a]	Sg [b] (m^2g^{-1})	PV [c] (cm^3g^{-1})	PS [d] (nm)	NiO CS [e] (nm)	H_2 uptake in TPR (μmol)	Coke (%)
SiO_2/500	593	1.5	8.9	-	--	--
SiO_2/900	184	0.4	7.1	-	--	--
SiNi/500	498	1.4	10.4	7.2	--	--
SiNi/900	330	1.1	10.3	7.4	44.2	1.2
SiNiCa/500	324	0.8	8.1	6.1	--	--
SiNiCa/900	132	0.4	8.1	6.8	46.3	0.31
SiNiMg/500	346	1.0	9.0	7.9	--	--
SiNiMg/900	183	0.5	9.3	8.2	47.5	0.06

[a]The number indicates the heating temperature in ^oC; [b]Specific surface area; [c]Total pore volume; [d] Average pore size; [e]CS, crystallite size, estimated from XRD according to Scherrer's equation.

Fig. 1(b) shows the TPR profiles of the catalysts calcined at 900 ^oC. All samples showed a reduction peak at high temperatures (700-800 ^oC), indicating that nickel oxide nanoparticles are interacting strongly with silica [12]. This is confirmed by the total hydrogen consumed in each case (Table 1) which was lower than the theoretical value (around 118 μmol) calculated considering the total reduction of nickel. The addition of calcium and magnesium slightly shifted the curve to lower temperature and also decreased the hydrogen uptake, indicating that both metals decreased the interaction of nickel with the support.
Fig. 2(a) shows the methane conversion as a function of time over the catalysts. The SiNi and SiNiCa samples were quite stable during reaction while the SiNiMg showed a light decrease. These results are in accordance with the low amounts of coke, produced on the catalysts as shown in Table 1. The most active catalyst was the magnesium-containing sample (70%) followed by the calcium-doped one (45%) which is more active than the undoped sample (30%). The selectivity to hydrogen followed the same tendency (Fig. 2). High amounts of hydrogen were produced over the doped samples, especially on the magnesium-doped one; however, these solids produced low amounts of carbon monoxide, showing that they are suitable for producing hydrogen rather than to produce syngas. These results are in accordance with previous works [13,14], using alumina-supported nickel, according to which the alkaline earth oxides are able to provide lower support acidity, higher nickel dispersions and better steam activation. This causes a high amount of the active sites available during reaction, by the inhibition of metal surface blocking by coke deposition, increasing the methane conversion.The magnesium-doped catalyst was the most suitable one for methane reforming, due to the high ability of magnesium in preventing coke, as stated earlier [15].

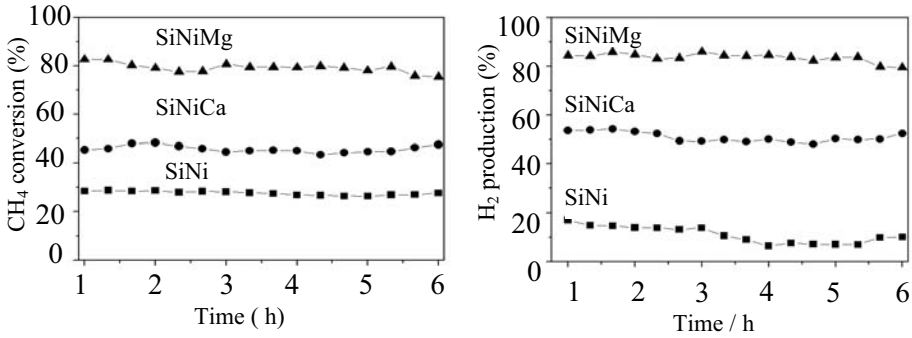

Figure 2. (a) Methane conversion and (b) hydrogen produced on the samples during the methane steam reforming. SiNi (square), SiNiCa (circle) and SiNiMg (triangle).

4. Conclusions

Silica-supported nickel prepared by the sol-gel method modified with citric acid is a promising catalyst to methane steam reforming. The addition of calcium and magnesium decreases the specific surface area but increases the activity and the selectivity to hydrogen. Magnesium-based catalyst showed the highest activity and selectivity of hydrogen and produced low amounts of carbon monoxide being suitable for hydrogen production.

5. References

[1] A. Fonseca, E. M. Assaf, J. Power Sour, 142 (2005) 154.
[2] R. Takahashi, S. Sato, T. Sodesawa, S. Tomiyama, Appl. Catal. A Gen. 286 (2005) 142.
[3] S. Tomiyama R. Takahashi, S. Sato, T. Sodesawa, S. Yoshida, Appl. Catal. A Gen. 241 (2003) 349.
[4] R. Takahashi, S. Sato, T. Sodesawa, M. Suzuki, N. Ichikumi, Micropor. Mesopor. Mater 66 (2003) 197.
[5] R.Takahashi,S.Sato,T.Sodesawa,M. Kawakita, K.Ogura, J. Phys. Chem. B 104 (2000) 12184.
[6] D. W. Lee, S K. Ihm. K. H. Lee, Micropor. Mesopor. Mater. 83 (2005) 262.
[7] B. D. Cullity, Introduction to Magnetic Materials, Addison-Wesley, Canada, 1972, p.181.
[8] K. Nakamoto, Infrared and Raman Spectra of Inorganic and Coordination Compounds, John Wiley & Sons: Canada, 1986.
[9] J. L. Bellamy, The infrared spectra of complex molecules, Chapman and Hall, London, 1975.
[10] F.F. Castillon, N.Bodganchikava, S. Fuentes, M..A.Borja, Appl. Catal. A Gen.175 (1998) 55.
[11] J. B. E. Caillerie, M. Kermarec, O. Clause, J. Phys. Chem. 99 (1995) 17273.
[12] B. Mile, D. Stiling , M.A Zammitt, , A. Lovell, M. Webb, J. Catal. 144 (1988) 217.
[13] J. T. Richardson, B. Turk, M. V. Twigg, Appl.Catal. A: Gen (1996) 97.
[14] J. de Lisboa, D.C.R.M Santos, F.B.Passos, F.B.Noronha, Catal. Today 101 (2005) 15.
[15] G. Xu, K. Shi, Y. Gao, H. Xu, Y. Wei, J. Molc. Catal. A: Chemical 147 (1999) 47.